International Journal of Adhesion & Adhesives 47 (2013) 91–98

Contents lists available at ScienceDirect

International Journal of Adhesion & Adhesives

journal homepage: www.elsevier.com/locate/ijadhadh

Mechanical characterization of a high elongation and high toughness epoxy adhesive

D.F.S. Saldanha [a,b], C. Canto [a,b], L.F.M. da Silva [a,*], R.J.C. Carbas [a,b], F.J.P. Chaves [a,b], K. Nomura [c], T. Ueda [c]

[a] Departamento de Engenharia Mecânica, Faculdade de Engenharia, Universidade do Porto, Rua Dr. Roberto Frias s/n, 4200-465 Oporto, Portugal
[b] Instituto de Engenharia Mecânica (IDMEC) – Pólo FEUP, 4200-465 Oporto, Portugal
[c] Nagase Chemtex, 1-1-17, Shinmachi, Nishi-ku, Osaka 550-8668, Japan

ARTICLE INFO

Available online 31 August 2013

Keywords:
Epoxides
Novel adhesive
Mechanical properties of adhesives
High toughness adhesive

ABSTRACT

In this paper, a new epoxy adhesive has been mechanically characterized. The adhesive combines the properties of an epoxy adhesive and typical polyurethane (PU) adhesive, such as high elongation and high toughness. Experimental tests were performed to measure the tensile properties, shear properties, thermal properties and fracture properties. The tensile test shows high tensile strength and high elongation. The single lap joint (SLJ) test shows that the failure load is proportional to the overlap length for hard steel adherends. For the SLJs with mild steel adherends, the failure occurred due to adherend yielding. Impact tests were conducted using SLJ specimens and the results are consistent with the SLJ tested under static conditions. The Tg was obtained using a Dynamic Mechanical Analysis (DMA) type of test. The toughness in mode I was determined using the Double Cantilever Beam (DCB) test and the toughness in mode II using End Notched Flexure (ENF) test.

1. Introduction

Epoxy adhesives are one of the most used in structural applications due to their high strength. One example is the automobile industry. In recent years due to the investigation and improvement of epoxy adhesives new techniques and concerns have arisen in the production of an adhesive joint. Where before little or no attention was given to joint design presently parameters such as joint surface, environment, work temperature and stress loads must be considered. Furthermore, for the automotive industry, under impact load it is crucial to transfer the load to the steel without fracturing the joint thus assuring the integrity of the car under a crash situation. However, pure epoxy adhesives are very brittle [3].

There is already some research on enhancing toughness without a major decrease in strength by adding rubber particles to epoxy adhesives. As a result of this investigation there are several types of rubber-modified epoxy resins with different sizes, shapes and compositions. These characteristics affect the toughness of the adhesive [4,5]. Other examples are the use of silica nanoparticles [6] and the mixing of two resins, where one of the resins is more flexible and increases the toughness of the system (e.g. epoxy-urethane system) [3].

More recently, crash resistant adhesives have been developed which give an even better toughness than the conventional toughened epoxies. These adhesives are particularly relevant to the automotive industry which is often subjected to impact loads. These adhesives have impact resistance and deform significantly without breaking, absorbing enough energy to keep the parts together [3]. These adhesives combine the high toughness of polyurethane and the high strength of an epoxy.

A new crash resistant epoxy adhesive has recently been developed by the Japanese adhesive manufacturer NAGASE CHEMTEX® (Osaka, Japan). The objective of this work is to study its mechanical behaviour and compare it to conventional toughened epoxies and polyurethane adhesives. Strength and fracture toughness tests were performed: bulk tensile test, single lap joint (SLJ) test, dynamic mechanical analysis (DMA) type test, double cantilever beam (DCB) test and end notched flexure (ENF) test. The bulk tensile test was used to evaluate the tensile strength and strain of the adhesive. SLJ tests were used to determine the shear strength in a joint. In order to assess the influence of overlap length three types of lengths were used (12.5, 25 and 50 mm). The adhesive thickness was 0.2 mm. The glass transition temperature, *Tg*, influences greatly the adhesives behaviour and in service the adhesive should work always below it in order to not be compromised [7]. This property was determined using a vibration apparatus through a Dynamic mechanical analysis (DMA) type of test.

* Corresponding author. Tel.: +351 22 508 17 06; fax: +351 22 508 14 45.
E-mail address: lucas@fe.up.pt (L.F.M. da Silva).

0143-7496/$ - see front matter © 2013 Elsevier Ltd. All rights reserved.
http://dx.doi.org/10.1016/j.ijadhadh.2013.08.001

Finally, the adhesive toughness was assessed by DCB and ENF tests which are necessary for the fracture characterization. The DCB test was used to measure the Mode I fracture toughness and the ENF test was used to measure the Mode II fracture toughness.

2. Experimental procedure

2.1. Materials

2.1.1. Adhesive

The epoxy adhesive XNR6852 was used, supplied by NAGASE CHEMTEX® (Osaka, Japan). This adhesive is a one-part system that cures at 150 °C for 3 h. This adhesive has a linear structure, which gives greater freedom of movement to the chains, unlike the network structure of a conventional epoxy adhesive. Along with the development of this adhesive, NAGASE CHEMTEX® has produced others with the same technique. The epoxy resin of XNR6852 when pure is a conventional thermosetting resin due to generating cross-linking during polymerization. A technological advance in the epoxy adhesive has been done and a no cross-linking polymer has been produced through the introduction of phenols. Thus the reaction process is changed and in this new process the epoxy resin and phenol are polymerized linearly by a consecutive reaction getting a no cross-linking polymer. As a consequence this polymer has some features of thermoplastic polymers due to the resulting linear structure [8].

2.1.2. Substrates

In the DCB and ENF tests, high tensile strength steel (DIN 40 CrMnMo 7) was used to avoid plastic deformation of the substrates. On the other hand for SLJ both hard (DIN C60) quenched in oil and ductile steel (DIN St33) were used in order to study the effect of adherend yielding on the joint strength. The general properties of the steels used are presented in Table 1.

The joint surface of all substrates was grit blasted and degreased with acetone prior to the application of the adhesive.

2.2. Tests

2.2.1. Bulk tensile test

The geometry of the bulk tensile test specimen is given in Fig. 1 according to BS 2782 standard [9]. The bulk tensile specimens were produced by curing the adhesive between steel plates of a mould (Fig. 2) with a silicone rubber frame according to the French standard NF T 76–142, which were hot pressed (2 MPa) for 3 h at 150 °C. A silicone rubber frame was used to avoid the adhesive from flowing out. The dimensions of the adhesive plate after cure were defined from the internal dimensions of the silicone rubber frame. Then, dogbone specimens were machined from the bulk sheet plates.

The bulk tensile test was performed in an INSTRON® model 3367 universal test machine with a capacity of 30 kN (Norwood, Massachusetts,USA), at room temperature and constant displacement rate of 1 mm/min. An extensometer to record the displacement was also used. Loads and displacements were recorded up to failure. Four specimens were tested.

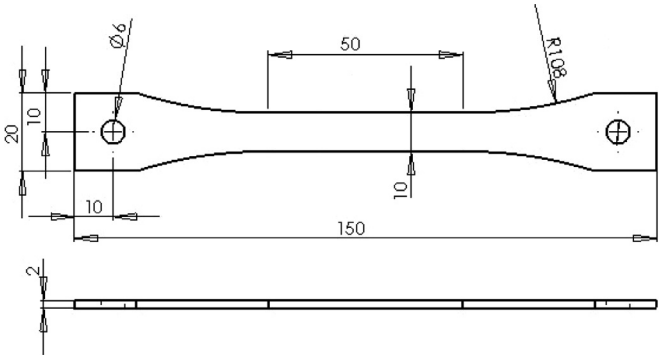

Fig. 1. Geometry of the bulk tensile test specimen (dimensions in mm).

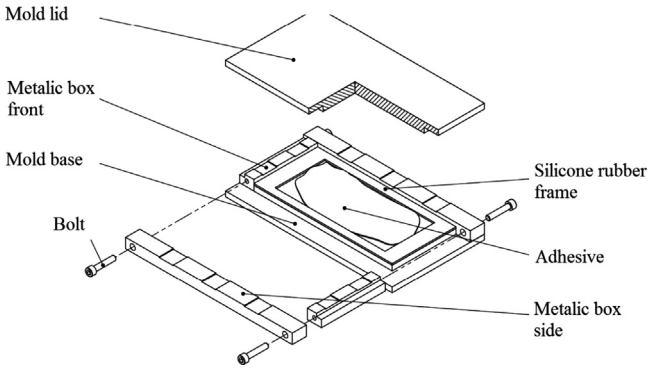

Fig. 2. Exploded view of the mould to produce plate specimens under hydrostatic pressure.

Table 1
Properties of the materials used for the adherends.

	Young's modulus (GPa)	Yield strength (MPa)	Tensile strength (MPa)	Strain (%)
DIN St33	205	183.8	288	17.6
DIN C60	205	1078	–	–
DIN 40 CrMnMo 7	205	895.5 ± 34.5	1034 ± 34	15.5 ± 1.5

2.2.2. Single lap joint (SLJ) test

Two different geometries were used. The geometry for SLJ test specimen with hard steel adherends is given in Fig. 3 and for the mild steel adherends in Fig. 4. By attaching two steel plates at the end of the SLJ specimen with mild steel there is improved grip during the test. The joint surfaces were grit blasted and degreased with acetone prior to the application of adhesive. After the surface preparation various overlaps were constructed (12.5, 25 and 50 mm) to assess the effect of the overlap on the joint strength. The thickness of the adhesive bond line was not studied and it was used 0.2 mm for it is believed that this value has little effect on the maximum adhesive joint strength. All the joints were manufactured without a fillet. For convenience it is repeated here that two materials were used a ductile steel (St33) and a high strength steel (C60) and the properties are presented in Table 1. The objective is to study its effect on the adhesive joint strength and failure mode.

A mould with spacers for correct alignment of the substrates was used to produce the SLJ specimens (Fig. 5). The substrates were bonded and the joints left under 2 MPa pressure for 3 h at 150 °C in a hydraulic hot plates press, being removed from the mould along with any excess adhesive at the end of the curing process.

The SLJ test was performed using a MTS® model 312.31 servo-hydraulic with a capacity of 250 kN (Eden Prairie, Minnesota, USA), machine at room temperature and at a constant displacement rate of 1 mm/min, according to standard ASTM D1002-99. A load cell of 250 kN was used. Loads and displacements up to failure were recorded. Three specimens of each overlap length were tested.

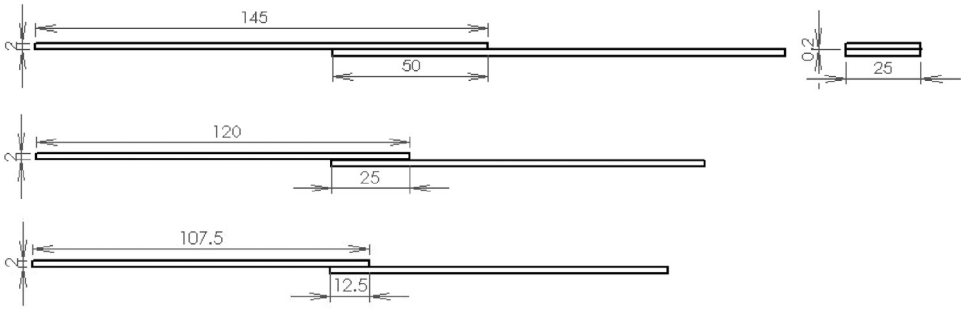

Fig. 3. Geometry of the SLJ test specimens with hard steel adherends (dimensions in mm).

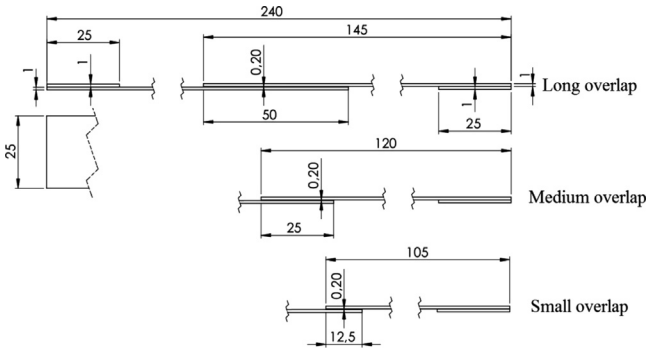

Fig. 4. Geometry of the SLJ test specimens with mild steel adherends (dimensions in mm).

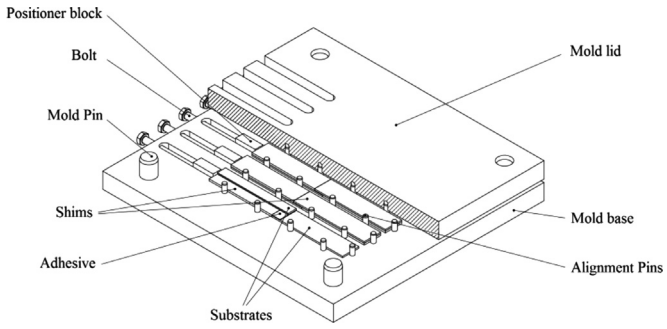

Fig. 5. Schematic mould for SLJ specimens.

2.2.3. Impact test

The same geometry of the long SLJ specimen (Fig. 4) and same fabrication procedure was used. This geometry was chosen because it is usually used and will therefore enable comparison with other academic work and because it is representative of a structural part.

The tests were conducted in Rosand® Intrumented Falling weight impact tester, type 5 H.V. (Stourbridge, West Midlands, U. K.). The machine is calibrated to give energy at impact of 300 J loading the specimen in tension. The energy was dissipated in the specimen from a falling mass of 29.83 kg with a velocity approximately equal to 4.47 m/s.

2.2.4. DMA type test

The glass transition temperature of the adhesive was measured using a DMA type apparatus based on a method with a vibrating beam at resonance [10,11]. In this method, a constrained layer vibrates at resonance and the temperature and amplitude are recorded.

From the theory of forced vibration, the damping is proportional to the inverse of the amplitude. In other words, when the amplitude is at its minimum the damping is at its maximum. The exact value of the damping is not needed, but just the temperature at which it peaks. The resonance frequency varies with temperature (the modulus and the dimensions of the specimen change) so it is necessary to ensure that the specimen is constantly at resonance using manual or automatic tuning (Fig. 6).

The samples were made of an aluminium beam, a central layer of adhesive and a plate on top to maximize damping. A mould was used to produce the specimens (Fig. 7). Firstly the plate is placed in the mould then the adhesive is applied and the beam is placed in the middle. Each mould can produce four specimens and the outer two have a thermocouple inserted. The specimen with thermocouple was used like a reference specimen to measure the temperature of the adhesive.

2.2.5. Double cantilever beam (DCB) test

The geometry of the DCB test specimen is given in Fig. 8. For the preparation of the specimens firstly the surface of the substrates was grit blasted and degreased with acetone prior to the application of adhesive. To guarantee the adhesive bondline thickness, spacers were inserted between the adherends on both ends. On one end two steel plates and a razor blade of 0.05 mm was inserted to introduce a pre-crack and guarantee a cohesive propagation from the beginning of the test. On the other end two steel plates were used making a thickness of 0.2 mm. Adhesive was applied in both adherends before assembly and were set in a mould for correct alignment while curing. The mould for DCB specimens was the same produced for the SLJ test specimens (Fig. 5). Lastly the joints were left under 2 MPa pressure for 3 h at 150 °C in a hydraulic hot plates press. After curing the DCB test specimens the spacers were removed along with any excess adhesive.

The specimen was tested according to standard ASTM D3433 in a MTS® model 312.31 servo-hydraulic with a capacity of 250 kN (Eden Prairie, Minnesota, USA), at room temperature and at a constant displacement rate of 0.5 mm/min. The specimen was loaded, as shown in, to measure the behaviour of the adhesive to fracture mode I. Pictures were recorded during the testing with 5 s intervals using a 10 MPixel digital camera. These images allowed the measuring of the crack length during its growth.

To calculate the critical fracture energy in mode I, G_{IC}, three different methods were used:

2.2.5.1. Compliance calibration method (CCM). Through this method, critical fracture energy is obtained using this equation:

$$G_{IC} = \frac{P^2}{2b}(3C_3a^2 + 2C_2a + C_1) \quad (1)$$

This technique is based on the Irwin–Kies equation [12]:

$$G_{IC} = \frac{P^2 dC}{2bda} \quad (2)$$

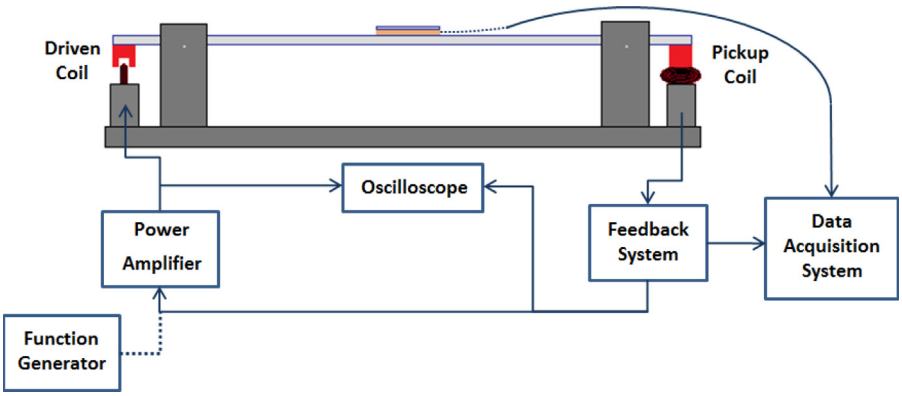

Fig. 6. Diagram of feedback circuit to maintain resonance.

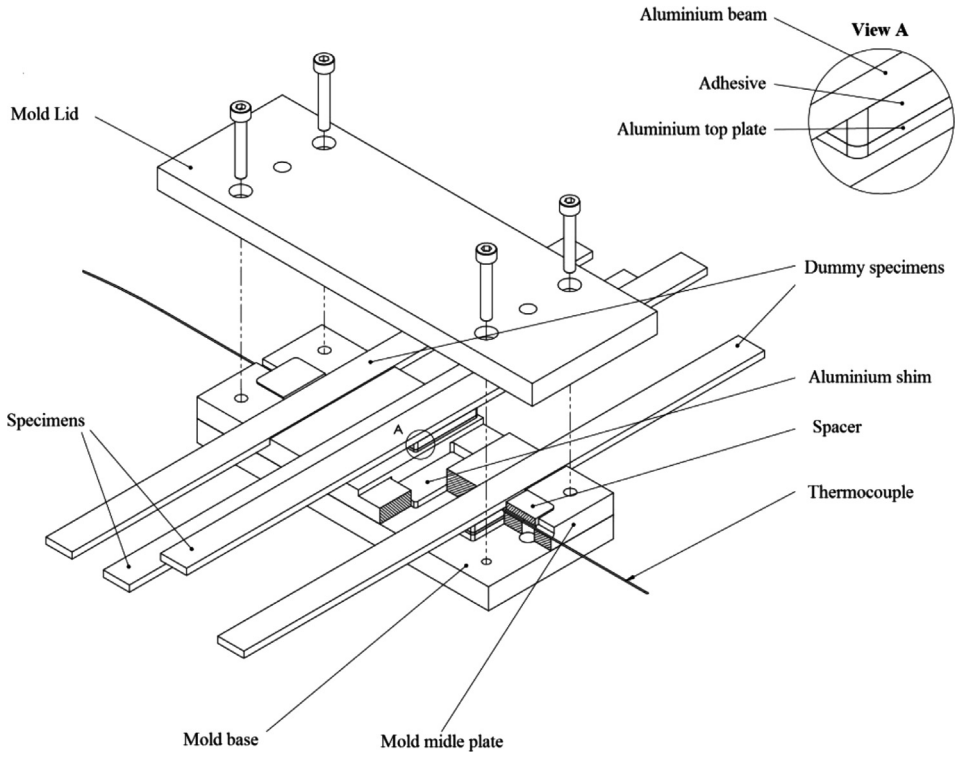

Fig. 7. Mould for the DMA type test specimen fabrication.

In this equation P represents load, b the specimen width, C the compliance, a the crack length and the $C=f(a)$ curves are fitted by cubic polynomials ($C=C_3a^3+C_2a^2+C_1a+C_0$).

2.2.5.2. Corrected beam theory (CBT). In this method the equation used is [13]:

$$G_{IC}=\frac{3P\delta}{2b(a+|\Delta|)} \tag{3}$$

here the crack tip rotation and deflection is taken into account, so Δ is used as a crack length correction.

2.2.5.3. Compliance-based beam method (CBBM). Although in other methods crack length measurement is necessary, here by using the crack equivalent concept this measurement is irrelevant depending only on the specimen's compliance during the test, using the equation below [14,15]:

$$G_{IC}=\frac{6P^2}{b^2h}\left(\frac{2a_{eq}{}^2}{h^2E_f}+\frac{1}{5G}\right) \tag{4}$$

where a_{eq} is an equivalent crack length obtained from the experimental compliance and accounting for the fracture process zone (FPZ) at the crack tip, E_f is a corrected flexural modulus to account for all phenomena affecting the P–δ curve, such as stress concentrations at the crack tip and stiffness variability between specimens, and G is the shear modulus of the adherents [9].

2.2.6. End notched flexure (ENF) test

The geometry used for the ENF test specimen is the same that was employed for the DCB test specimen (Fig. 8) and the same surface treatment was applied. The specimen was tested in a MTS 312.31 servo-hydraulic machine at room temperature and at a constant displacement rate of 0.5 mm/min. A load cell of 250 kN was used. In order to avoid a blunt crack and ensure the crack

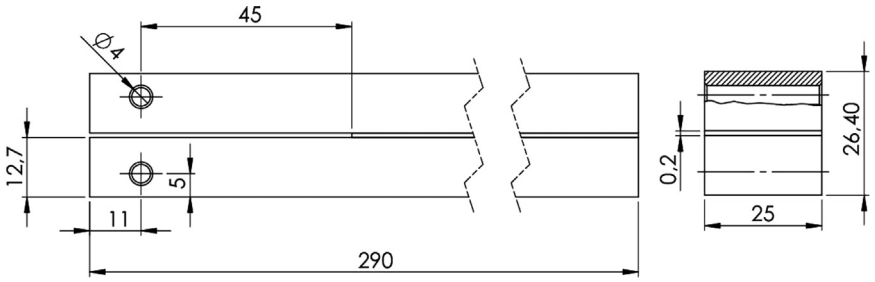

Fig. 8. Geometry of the DCB specimen (dimensions in mm).

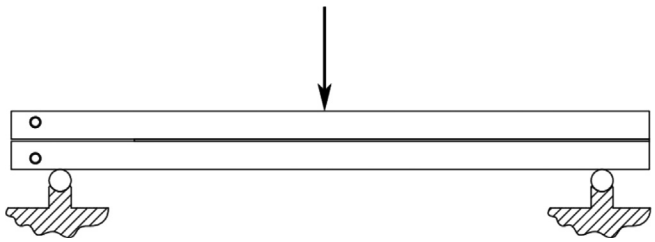

Fig. 9. End Notched Flexure (ENF) test.

propagation, the specimens were lightly loaded in mode I before the beginning of the test. As shown in Fig. 9, the specimen is subjected to bending in three points leading to mode II fracture in the adhesive.

The Compliance-Based Beam Method (CBBM) was used to evaluate the G_{IIC}. The accurate measurement of the crack length makes the evaluation of critical fracture energy in mode II, G_{IIC}, very difficult. This happens because in this test the two substrates are pressed against each other. This method does not require measurement of the crack length, and is based on the crack equivalent concept, depending only on the specimen's compliance. Moreover, unlike when the real crack length is considered, the equivalent crack length (a_{eq}) takes into account the FPZ effects at the crack tip. The following equation is used [16–18]:

$$G_{II} = \frac{9P^2 a_{eq}^2}{16 b^2 E_f h^3} \quad (5)$$

where P is load, E_f is an equivalent flexural modulus, a_{eq} is the equivalent crack length, b is the specimen width and h is the adherend thickness. The E_f is calculated from the initials crack length and compliance to avoid the influence of specimen variability on the results.

3. Results and discussion

3.1. Bulk tensile test

Young's modulus obtained is approximately half of a typical toughened epoxy (Table 2) and it is a consequence of the addition of the phenols. This property can have some advantages to the vibration damping [19] because of its smaller rigidity.

The values of tensile strength determined in this test correspond to the values expected for a conventional epoxy adhesive (Table 2). However, the elongation value is much higher than a conventional toughened epoxy adhesive and the strength is higher than a polyurethane adhesive. In Figs. 10 and 11 can be seen the comparison of a tensile curve between toughened epoxy, AV 119 from Hunstman®, a polyurethane, Pliogrip 7400/7410 from Ashland Specialty Chemicals®, and the studied adhesive, XNR 6852. Before fracturing the adhesive deforms in a ductile manner suffering a reduction of area and acquiring an opaque colour

Table 2
Results of bulk tensile tests.

	Tensile strength (MPa)	Young's modulus (MPa)	Strain (%)
XNR6852	59.9 ± 0.84	1176.3 ± 39.9	100.7 ± 25.52
AV 119	60	2400	3

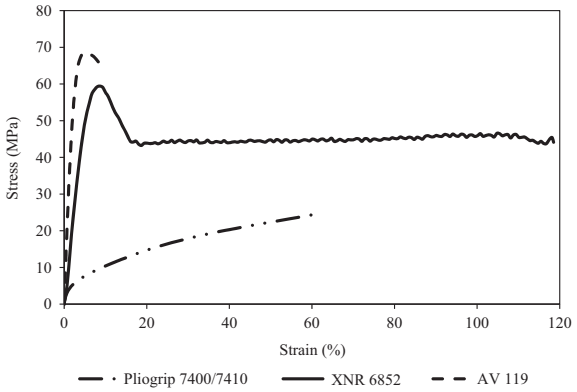

Fig. 10. Stress–strain curve with, Pliogrip 7400/7410 (PUAV 119) [1], (toughened epoxy) [2] and XNR6852.

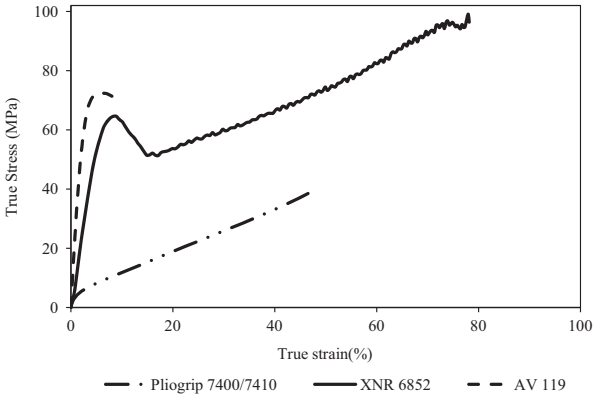

Fig. 11. True Stress-True strain curve with, Pliogrip 7400/7410 (PU) [1], AV 119 (toughened epoxy) [2] and XNR6852.

(Fig. 12), behaviour typical of thermoplastic polymers. This behaviour is an improvement in the properties of epoxy adhesives demonstrating an increased ductility of the material.

3.2. Single lap joint (SLJ) test

Two different adherends were tested. The first, a hard steel for the SLJ specimens, and in this case it failed cohesively with an irregular and whitening of the adhesive, indicating plastic deformation in the adhesive, as shown in Fig. 13. Also for the hard steel

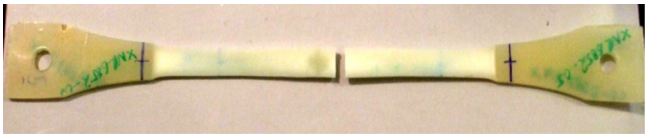

Fig. 12. Bulk tensile specimen after test.

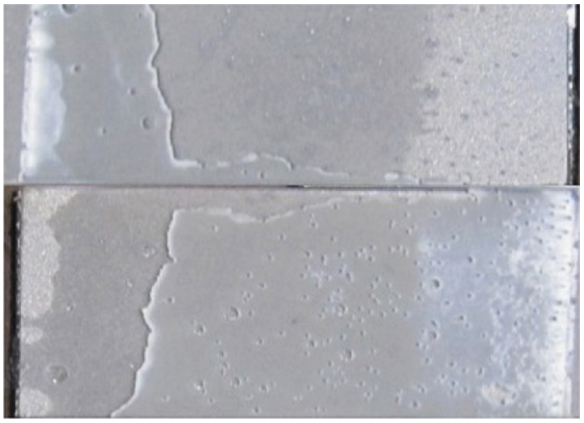

Fig. 13. SLJ specimen fracture surface.

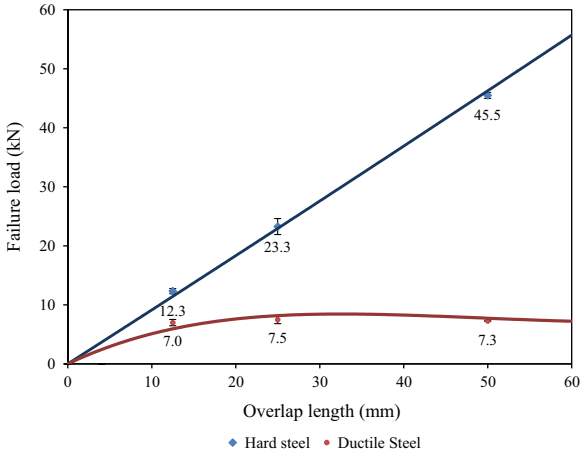

Fig. 14. Failure load (kN) vs. overlap length (mm).

adherends the failure loads increased linearly with the overlap length (Fig. 14) behaviour typical of a highly ductile adhesive which develop uniform load transfer over the joint length [19]. A conventional epoxy adhesive usually has a rather brittle behaviour which does not permit the adhesive to deform plastically all over the overlap. The failure strain of the adhesive is reached at the ends of the overlap before there can be global yielding of the adhesive along the whole overlap [20,21]. In this case, we can observe that the global yielding criteria of the adhesive work perfectly because this adhesive has a ductile behaviour.

The average lap shear strength (τ_{av}) is given by: $\tau_{av} = P/bL = 39.25 \pm 1.63$ MPa, where P is the maximum load, b is the joint width and L is the joint overlap length.

On the other hand the ductile steel adherends were also tested. In previous studies, as example the work done by Karashalios [22], when using a mild steel failure is dominated by local strain at the edge of the overlap. Contrary to typical epoxy adhesives the present study has shown a different behaviour, in this case the failure was always on the adherends and the exception was only for the low overlap where both adherend failure and cohesive failure was observed. Although rupture occurs in the steel the adhesive is still damaged in the edge of the overlap.

For the mild steel the load to failure is directly correlated to the tensile strength of the steel adherend as can be observed by the plateau in Fig. 14. From a mean value of 7.15 kN observed in the SLJ test the stress in the adherend is of 286 MPa similar to the tensile strength in Table 1 of DIN St33.

3.3. Impact test

The rupture was in all cases in the steel adherends. Under high strain rate the same failure mode as in the quasi-static tests was obtained and again a case of plane stress was observed in the steel adherend. Due to the high strain rate the steel adherends had a different behaviour deforming less and absorbing less energy when comparing with the quasi-static test (Table 3 and Fig. 15). As a result of the strain rate dependence of the steel the failure load was increased but the adhesive experienced a similar damage as in the case of static loading. For application where impact energy absorption is important well-constructed adhesive joints with a high elongation epoxy such as the studied is interesting for it has a high damage tolerance, high elongation and high strength.

3.4. Dynamic mechanical analysis (DMA) test

The *Tg* value corresponding to the peak of damping was found to be 102.6 ± 0.1 °C. This value is similar to the indicated by the manufacturer. In Fig. 16, the peak corresponds to the temperature of maximum damping (1/Amplitude).

For some applications in automotive industry, the *Tg* should be above 80 °C to avoid a strong change in the modulus of the adhesive at the work temperature [7]. Considering that, this adhesive has an appropriate *Tg* for this application.

3.5. Double cantilever beam (DCB) test

As can be observed in Fig. 17, the failure in the DCB specimens was cohesive. The critical fracture energy in mode I, G_{IC}, was evaluated using the methods described in Section 2.2.5 (CCM, CBT

Table 3
Energy (J) and failure load (N) values obtained from the quasi-static and impact test.

	Energy (J)	Failure load (kN)
Quasi-static test	291.64 ± 22.17	7.26 ± 0.04
Impact test	260.09 ± 7.69	12.22 ± 0.57

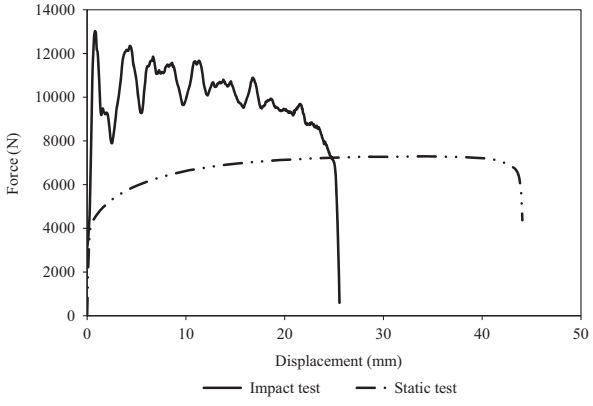

Fig. 15. Comparison of SLJ with mild steel adherends under two different strain rates. The first an impact test and the second a quasi-static load.

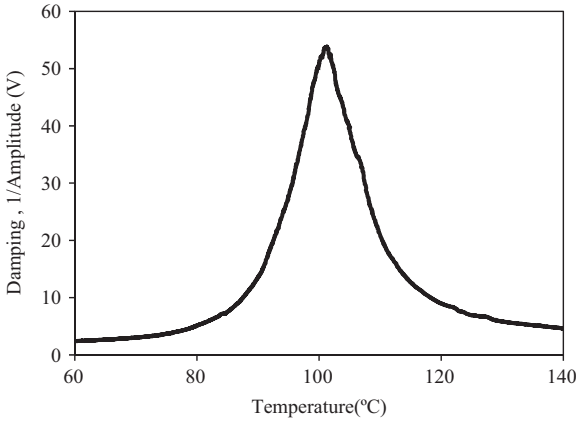

Fig. 16. Damping (1/amplitude) vs. temperature obtained in the DMA type test.

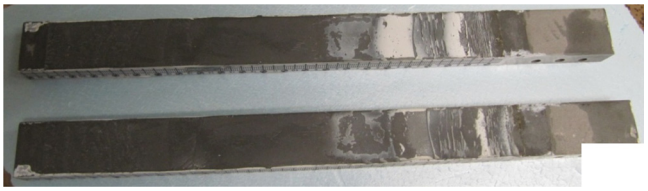

Fig. 17. Failure surface of a DCB specimen in mode I.

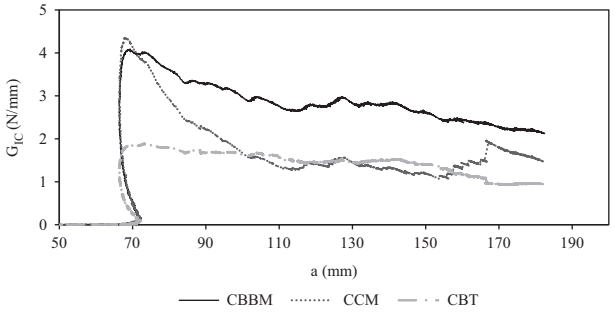

Fig. 18. Experimental R-curve obtained for the DCB test.

Table 4
Values obtained for the mode I fracture toughness using three different methods, CBBM, CCM, CBT.

	CBBM	CCM	CBT
G_{IC} (N/mm)	2.21 ± 0.49	1.77 ± 0.37	1.94 ± 0.29

and CBBM). An example of the R-curves obtained by the three methods is shown in Fig. 18. It is possible to observe an initial increase of G_{IC} corresponding to the crack blunting effect followed by a plateau. This plateau was used to identify the fracture energy.

The average G_{IC} from the three techniques employed can be seen in Table 4. The final value of 1.97 N/mm (value determined using an average of the techniques) is much higher than conventional toughened epoxy adhesives (0.3–0.6 N/mm) and comparable to that of a polyurethane adhesive (1.2–2.9 N/mm) [21].

3.6. End notched flexure (ENF) test

One typical R-curve obtained with this test is shown in Fig. 19. A plateau is clearly seen indicating stable crack propagation. An average G_{IIC} value of 12.5 ± 1.1 N/mm was obtained. This value is similar to the G_{IIC} of ductile adhesives [23] as previously observed in mode I.

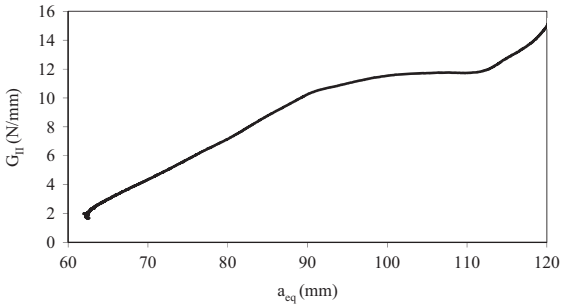

Fig. 19. Experimental R-curve obtained for the ENF test.

Relating the values of G_{IC} and G_{IIC} for this adhesive makes a relation G_{IIC}/G_{IC} of approximately 5.2. This value is comparable to that obtained with other epoxy adhesives although the relation varies greatly. Relation between 5 and 10 are documented in the literature [16,23,24].

4. Conclusion

This work aimed to determine the mechanical properties of the novel epoxy adhesive, XNR 6852, evaluating the applicability of this adhesive in the automotive industry by the relation between strength and toughness. The tests realized have shown that the new adhesive has:

1 High tensile strength (approximately 60 MPa), typical of an epoxy adhesive.
2 High elongation (approximately 100%), typical of a polyurethane adhesive.
3 High shear strength (approximately 40 MPa in a SLJ), typical of an epoxy adhesive.
4 A linear relation between failure load and overlap length in SLJs showing a ductile behaviour.
5 Can withstand deformation and damage without a brittle behaviour for both impact and quasi-static cases.
6 High toughness (G_{IC} = 1.97 N/mm and G_{IIC} = 12.5 ± 1.1), typical of a polyurethane adhesive.

In short, this novel adhesive (XNR6852) combines the best properties of epoxy and polyurethane adhesives being a great solution for the automotive industry.

Acknowledgements

The authors would like to thank NAGASE CHEMTEX® (Osaka, Japan) for the information provided and the supplying of the epoxy adhesive XNR6852.

References

[1] Kelly G. Quasi-static strength and fatigue life of hybrid (bonded/bolted) composite single-lap joints. Composite Structures 2006;72:119–29.
[2] Karachalios EF, Adams RD, da Silva LFM. Single lap joints loaded in tension with high strength steel adherends. International Journal of Adhesion and Adhesives 2013;43:81–95.
[3] Silva LFMd, Öchsner A, Adams RD. Handbook of adhesion technology. 1st ed. Berlin: Springer; 2011.
[4] Imanaka M, Motohashi S, Nishi K, Nakamura Y, Kimoto M. Crack-growth behavior of epoxy adhesives modified with liquid rubber and cross-linked rubber particles under mode I loading. International Journal of Adhesion and Adhesives 2009;29:45–55.

[5] Imanaka M, Takagishi M, Nakamura N, Kimoto M. R-curve characteristics of adhesives modified with high rubber content under mode I loading. International Journal of Adhesion and Adhesives 2010;30:478–84.
[6] Zhang H, Tang L-C, Zhang Z, Friedrich K, Sprenger S. Fracture behaviours of in situ silica nanoparticle-filled epoxy at different temperatures. Polymer 2008;49:3816–25.
[7] B B. Automotive industry, handbook of adhesion technology. Berlin: Springer; 1185–2212.
[8] T.Y. Tsujimura. High toughness composites based on insitupolymerizable thermoplastic epoxy-resin. In: 29th International Conference and Forum—SAMPE Europe SEICO 08, Paris; 2008.
[9] Banea MD, Silva LFMd, Campilho RDSG. Effect of temperature on tensile strength and mode I fracture toughness of a high temperature epoxy adhesive. Journal of Adhesion Science and Technology 2012;26:939–53.
[10] Guild FJ, Adams RD. A new technique for the measurement of the specific damping capacity of beams in flexure. Journal of Physics E: Scientific Instruments 1981;14:355.
[11] Zhang Y, Adams RD, da Silva LFM, Rapid A. Method of measuring the glass transition temperature using a novel dynamic mechanical analysis method. Journal of Adhesion 2013;89:785–806.
[12] M.F. Kanninen, C.H. Popelar. Advanced fracture mechanics. Oxford University Press, Oxford, 1985.
[13] Robinson P, Das S, Mode I. DCB testing of composite laminates reinforced with *z*-direction pins: a simple model for the investigation of data reduction strategies. Engineering Fracture Mechanics 2004;71:345–64.
[14] de Moura MFSF, Campilho RDSG, Gonçalves JPM. Crack equivalent concept applied to the fracture characterization of bonded joints under pure mode I loading. Composites Science and Technology 2008;68:2224–30.
[15] de Moura MFSF, Gonçalves JPM, Chousal JAG, Campilho RDSG. Cohesive and continuum mixed-mode damage models applied to the simulation of the mechanical behaviour of bonded joints. International Journal of Adhesion and Adhesives 2008;28:419–26.
[16] Banea MD, da Silva LFM, Campilho RDSG. Mode II fracture toughness of adhesively bonded joints as a function of temperature: experimental and numerical study. Journal of Adhesion 2012;88:534–51.
[17] da Silva LFM, Esteves VHC, Chaves FJP. Fracture toughness of a structural adhesive under mixed mode loadings Bruchzähigkeit eines Strukturklebstoffs bei Mixed-Mode Belastung. Materialwissenschaft und Werkstofftechnik 2011;42:460–70.
[18] de Moura MFSF, de Morais AB. Equivalent crack based analyses of ENF and ELS tests. Engineering Fracture Mechanics 2008;75:2584–96.
[19] Banea MD, da Silva LFM. Static and fatigue behaviour of room temperature vulcanising silicone adhesives for high temperature aerospace applications. Statisches Verhalten und Dauerfestigkeitsanalyse von vulkanisierten Silikonklebstoffen für Luftfahrtanwendungen bei hohen Temperaturen, Materialwissenschaft und Werkstofftechnik 2010;41:325–35.
[20] Banea MD, da Silva LFM. Mechanical characterization of flexible adhesives. Journal of Adhesion 2009;85:261–85.
[21] da Silva LFM, Carbas RJC, Critchlow GW, Figueiredo MAV, Brown K. Effect of material, geometry, surface treatment and environment on the shear strength of single lap joints. International Journal of Adhesion and Adhesives 2009; 29:621–32.
[22] Karachalios EF, Adams RD, da Silva LFM. Single lap joints loaded in tension with ductile steel adherends. International Journal of Adhesion and Adhesives 2013;43:96–108.
[23] da Silva LFM, de Magalhães FACRG, Chaves FJP, de Moura MFSF. Mode II fracture toughness of a brittle and a ductile adhesive as a function of the adhesive thickness. Journal of Adhesion 2010;86:891–905.
[24] da Silva LFM, Ramos JE, Figueiredo MV, Strohaecker TR. Influence of the adhesive, the adherend and the overlap on the single lap shear strength. Journal of Adhesion and Interface 2006;8.